Chinese Science Bulletin

Water-soluble chitosan nanoparticles as a novel carrier system for protein delivery

WANG Chun†, FU Xiong & YANG LianSheng

School of Light Industry and Food Sciences, South China University of Technology, Guangzhou 510640, China

High MW chitosan (CS) solutions have already been proposed as vehicles for protein delivery. The aim of the present work is to investigate the potential utility of water-soluble chitosan (WSC) as vehicles to load and deliver proteins. WSC nanoparticles (WSC NP) with various formations were prepared based on ionic gelation of WSC with pentasodium tripolyphosphate (TPP) anions. Bovine serum albumin (BSA) was used as a model protein drug incorporated into the WSC nanoparticles. Blank and BSA-loaded WSC nanoparticles were examined and determined to have a spherical shape with diameters between 35—190 nm, and zeta potential between 35—42 mV. FTIR confirmed that the tripolyphosphoric groups of TPP linked to the ammonium groups of WSC in the nanoparticles. Some factors affecting delivery properties of BSA have been investigated. Altering the concentration of BSA from 0.05 to 1 mg/mL enhanced the loading capacity of BSA but decreased loading efficiency simultaneously. Also, with the introduction of poly ethylene glycol (PEG), BSA release accelerated. Nanoparticle preparation from WSC with various deacetylation degrees (DDs) from 72.6% to 90% and MWs ranging from 3.5 to 15.8 kDa promoted loading efficiency and decreased the release rate. These results indicate that WSC nanoparticles are promising carriers for protein delivery.

water-soluble chitosan (WSC), nanoparticles, bovine serum albumin (BSA), protein delivery

1 Introduction

Chitosan [α (1→4) 2-amino 2-deoxy β-D-glucan], a cationic polysaccharide obtained from the deacetylation of chitin, has received wide attention as a pharmaceutical excipient because of its unique properties such as biocompatibility, biodegradability, low-immunogenicity and non-toxicity[1,2]. Besides other applications[3], chitosan has been extensively examined for its potential in the development of the controlled release drug delivery systems[4−7]. Also, nanoparticle chitosan is shown to be an attractive alternative to liposomes for the delivery of peptides, proteins, antigen, oligonucleotides and genes, since it has the advantages of longer shelf life and generally a higher drug carrying capacity[8]. However, in some fields especially in medicine and food industry, the application of chitosan is limited by its high MW resulting in low solubility in physiological solutions due to its crystalline structure[9]. Being insoluble in aqueous solutions, it is difficult to chemically modify in a neutral pH condition since chitosan is only dissolved in water containing acetic acid[9−12]. Also, there is a possibility of inducing cytotoxicity to sensitive bioactive macromolecules because of the use of acetic acid.

Water-soluble chitosan (WSC), including chitosan oligosaccharides (COS) and some low molecular chitosan (LMC), has been attracting increasing attention as a substitute for high MW chitosan due to its higher water solubility. Chae[13] reported the utilization of 2 different chitosan oligosaccharides (with the average molecular weight of 3 and 6 kDa) as a non-viral gene carrier for gene delivery, which showed great potential to be a gene carrier with a high level of gene transfection efficiencies even in the presence of serum. To increase the solubility

Received September 21, 2006; accepted November 21, 2006
doi: 10.1007/s11434-007-0127-y
†Corresponding author (email: awaw1112@yahoo.com.cn)

of chitosan in water and decrease the cytotoxicity induced by acetic acid, water-soluble chitosan (WSC, with the average molecular weight of 13 to 18 kDa) nanoparticles were prepared, which showed no cytotoxic effects on cells and a high transfection into HepG2[9]. However, water-soluble chitosan as a carrier for protein delivery has seldom been reported, and furthermore, some important factors affecting drug properties have not been investigated, for instance basic molecular parameters of water-soluble chitosan, molecular weight (MW) and deacetylation degree (DD) were not evaluated in drug delivery system of nanoparticles.

Chitosan nanoparticles are obtained by the process of ionotropic gelation based on the interaction between the negatively charged groups of the pentasodium tripolyphosphate (TPP) and the positively charged amino groups of CS. This process has been used to prepare CS nanoparticles for the delivery of peptides and proteins[14] including insulin[15] and cyclosporine[16].

Polyethylene glycol (PEG) has been widely used in biomaterial application. It is hydrophilic, flexible, nonionic and biodegradable. PEG-coated nanoparticles have been found to have substantial potential in therapeutic applications as an injectable colloidal system for controlled, and site-specific drug delivery[17−19].

Taking this into account, the purpose of the current study was to investigate water-soluble chitosan as a carrier system for protein delivery and some factors affecting drug delivery. Therefore, we investigated in detail the physicochemical properties of protein association to WSC and WSC/PEG nanoparticles that were made of different molecular weights and deacetylation degrees (DD) by using a very mild and friendly ionic gelation technique[20]. Finally, we analyzed the release behavior *in vitro* of these novel particles in order to establish their utility for the delivery of a model protein bovine serum albumin (BSA).

2 Materials and methods

2.1 Materials

Chitosan (hydrochloride salt) with a deacetylation degree (DD) of 90% and an MW of 200 kDa was supplied by Golden-Shell Biochemical Co. (Zhejiang, China). Water-soluble chitosan (WSC) with a DD of 90% and different MWs (3.5, 6.3, 10.1, 13.5, 15.8 kDa) and water-soluble chitosan with an MW of 6.3 KDa and different DDs (72.6, 84.2, 90.7%) were prepared according to refs. [21, 22]. The MWs were measured through gel permeation chromatography (GPC) while the DDs were determined by elemental analysis. Bovine serum albumin (BSA) with an MW of 68 kDa and pentasodium tripolyphosphate (TPP) were purchased from Sigma Chemical Co. (USA). Polyethylene glycol (PEG) with an MW of 20 kDa was bought from Tiantai Chemical Company (Tianjin, China). All other chemicals were of reagent grade.

2.2 Preparation of water-soluble chitosan (WSC) nanoparticles and BSA loaded nanoparticles

Water-soluble chitosan (WSC) nanoparticles were prepared according to the procedure first reported by Calvo et al.[20], based on the ionic gelation of WSC with pentasodium tripolyphosphate (TPP) anions. Water-soluble chitosan with various MWs and DDs was dissolved in deionized water (pH 7.4) at different concentrations. Under magnetic stirring at room temperature[23], a 1-mL aqueous solution of pentasodium tripolyphosphate (TPP) of various concentrations was added to a 5-mL water-soluble chitosan (WSC) solution, e.g. WSC 2 mg/mL and TPP 1 mg/mL, to get a WSC/TPP weight ratio of 10∶1. PEG-modified nanoparticles were formed spontaneously upon incorporation of the 1 mL TPP solution with the 5 mL chitosan solution containing PEG (0.25 mg/mL).

BSA-loaded nanoparticles were formed upon incorporation of a TPP solution with a chitosan solution containing various concentrations of BSA.

The detailed formation conditions are shown in the corresponding legends and figures.

2.3 Determination of nanoparticles process yield

The WSC nanoparticles production yield was calculated by gravimetry as described elsewhere[24]. Fixed volumes of nanoparticle suspensions were centrifuged (20000 rpm, 30 min, 15℃) and sediments were freeze-dried over 24 h (24 h at −30℃ and gradually warmed until 25℃), using a Labconco Freeze Dryer (Labconco, USA).

The process yield (PY) was calculated as follows:

$$\text{PY}(\%) = \text{Total nanoparticle weight}/\text{Total solids weight} \times 100. \quad (1)$$

2.4 Physicochemical characterizations of WSC nanoparticles

2.4.1 Measurement of particle sizes and zeta-potential. The average particles size and zeta potential of the

nanoparticles were determined by dynamic light scattering (DLS) with Autosizer 3000 (Malvern Instruments Limited, UK)[25] and a zeta potential analyzer (Brookhaven, USA), in triplicate respectively.

2.4.2 Transmission electron microscopy (TEM) studies. Nanoparticle morphology was observed using TEM (2010HR, JEOL, Japan). The samples were stained with 2% (*w/v*) phosphotungstic acid and placed on copper grids. And then they were dried at room temperature for 15 min, and then examined using a TEM.

2.4.3 Fourier transform infrared (FT-IR) spectral studies. WSC nanoparticles separated from suspension were dried by a freeze dryer, and their FT-IR was taken with KBr pellets on a Bruker VECTOR33 spectrometer (Germany).

2.5 Determination of BSA loading efficiency of nanoparticles

BSA loading efficiency of nanoparticles was determined according to the procedure by Xu et al.[27]. The loading efficiency and loading capacity of nanoparticles were determined by the separation of nanoparticles from the aqueous medium containing non-associated BSA by ultra-centrifugation at 20000 r/min, at 15℃ for 30 min. The amount of free BSA in the supernatant was measured by UV spectrophotometry at 280 nm using the supernatant of the non-loaded BSA nanoparticles as basic correction. A calibration curve was made with measuring the absorbances of the known BSA solution by spectrophotometry. The loading efficiency (LE) and the BSA loading capacity (LC) of the nanoparticles were calculated as follows:

$$\text{LE (\%)} = (\text{total BSA} - \text{free BSA})/\text{total BSA} \times 100, \quad (2)$$

$$\text{LC (\%)} = (\text{total BSA} - \text{free BSA})/\text{nanoparticles weight} \times 100. \quad (3)$$

2.6 *In vitro* release studies

The BSA release profiles of nanoparticles were determined as follows[26,27]. The BSA-loaded WSC nanoparticles (2 mg) separated from suspension were incubated in 4 mL of phosphate buffered saline (PBS) (0.2 mol/L, pH 7.4) at 37℃ under stirring. At predetermined time intervals, the samples were ultra-centrifuged, and 3 mL of supernatant was removed. The samples were supplemented with 3 mL of fresh release medium and resuspended. The study was conducted until significant aggregation of the particles occurred (10 d)[14]. The amount of BSA released was determined by modified Coomassie Brilliant Blue protein assay (Pierce, Inc, New York, NY, USA). The calibration curve was made as before and non-loaded nanoparticles were used to correct the intrinsic absorbance of WSC.

3 Results and discussion

3.1 Physicochemical characterizations of WSC nanoparticles

TEM of the nanoparticles and their surface morphology are shown in Figure 1. WSC-TPP nanoparticles (Figure 1(a)) and PEG-modified nanoparticles (Figure 1(b)) are spherical in shape. A similar morphology was also observed for BSA-loaded WSC-TPP nanoparticles (Figure 1(c)). The sizes of these nanoparticles are consistent with those determined by DLS.

Figure 2 shows FTIR spectra of WSC, WSC-TPP nanoparticles, BSA-loaded nanoparticles and BSA. There are three characterization peaks of WSC (Figure 2-b) at 3430 cm^{-1} from υ(OH), 1073 cm^{-1} from

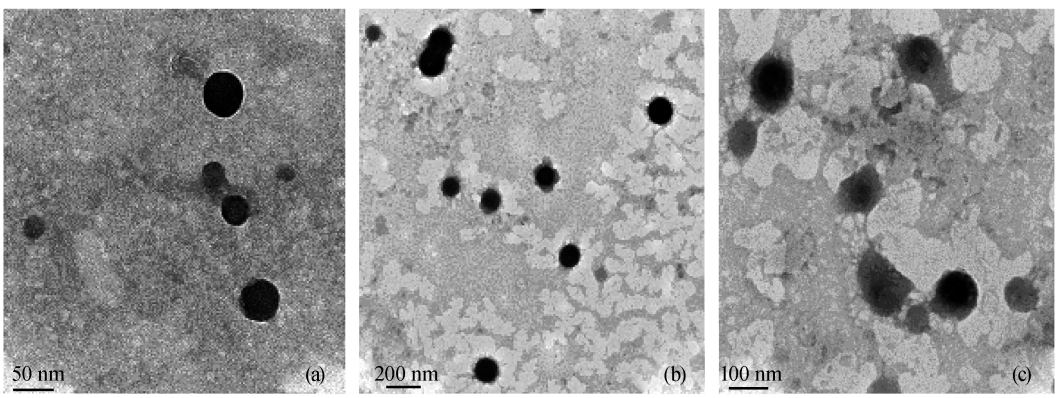

Figure 1 TEM of WSC (a), WSC/PEG (b) and BSA-loaded WSC-TPP nanoparticles (c) (WSC MW = 6.3 kDa, WSC 2 mg/mL, TPP 1mg/mL).

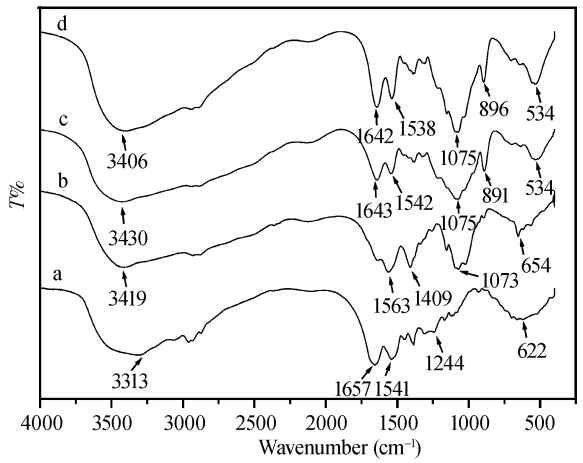

Figure 2 FTIR of (a) BSA, (b) WSC, (c) WSC nanoparticles, and (d) BSA-loaded nanoparticles (MW 6.3 kDa, DD 90%, WSC 5 mL 2 mg/mL, TPP 1 mL 1 mg/mL, BSA 0.1 mg/mL).

δ(C-O-C) and 1563 cm^{-1} from $\upsilon(NH_2)$. The spectrum of WSC-TPP nanoparticles (Figure 2-c) is different from that of a WSC matrix (Figure 2-b). In WSC-TPP nanoparticles, the peak of 3430 cm^{-1} becomes wider, indicating that hydrogen bonding is enhanced. In WSC-TPP nanoparticles, the 1563 cm^{-1}, peak of $-NH_2$ bending vibration shifts to 1542 cm^{-1} and a new sharp peak at 1643 cm^{-1} appears. The FTIR spectrum is consistent with the result of chitosan film modified by phosphate, and it could be attributed to the linkage between phosphoric and ammonium ions[28]. We presume that the tripolyphosphoric groups of TPP were linked with ammonium groups of the chitosan in the nanoparticles. Characteristic peaks of BSA have acetylamino I 1657 cm^{-1}, II 1541 cm^{-1} and III 1244 cm^{-1}, and 3313 cm^{-1} from $\upsilon(NH_2)$. Acetylamino I 1657 cm^{-1} and II 1541 cm^{-1} in BSA overlap 1643 cm^{-1} from δ(NH) and 1542 cm^{-1} in non-loaded WSC nanoparticles, so more intensive peaks of both are shown in BSA-loaded nanoparticles (Figure 2-d).

Table 1 shows the influence of WSC molecular weight on the process yield, the size and zeta potential values of the nanoparticles. A gradual increase in the particle size and process yield with an increase in molecular weight was noted, but no significant change was observed in the zeta potential.

Table 1 Process yields and physicochemical properties of blank (without BSA) nanoparticles prepared with different WSC molecular weight (mean ± S.D., $n = 3$)[a)]

MW of WSC	Process yield (%)	Size (nm)	Zeta potential (mV)
3500	28±3	71.2±8.2	38.4±1.7
6300	35±4	83.1±9.8	38.2±2.3
10,100	38±3	120.3±10.2	41.2±2.2
13,500	41±5	157.5±9.3	40.9±2.0
15,800	47±4	187.6±23	41.1±1.6

a) WSC to TPP mass ratio = 11:1, $T = 25\pm1$℃, pH = 7.4.

Nanoparticles (prepared with molecular weight 6.3 kDa WSC) with WSC/TPP ratios of 10:1—21:1 were obtained. When the WSC/TPP ratios were lower than 10:1 or higher than 21:1, a nanoparticle solution could not be formed because there was solution (at high WSC/TPP ratios) or aggregation formation (at low WSC/TPP ratios) (data not shown). The ratios of WSC/TPP to form nanoparticles are higher than the high molecular weight chitosan/TPP[24,29]. The results indicate that WSC associates less TPP to form nanoparticles compared with high molecular weight chitosan which suggests that there are more active amine groups exposed on the WSC molecular structure. Figure 1(a) displays the TEM microphotograph of representative fresh WSC-TPP nanoparticles, which show evidence of a compact structure. As shown in Table 2, the incorporation of increasing amounts of TPP with respect to WSC led to a significant increase in the loading efficiency (LE), and the maximum loading efficiency (approximately 68%) achieved for a 10:1 WSC/TPP ratio. It was stated that the highly viscous nature of the gelation medium hinders association of BSA in the study of chito-

Table 2 Physicochemical properties of blank (without BSA) and BSA-loaded nanoparticles prepared with different WSC/tripolyphosphate (WSC/TPP) theoretical ratios (mean ± S.D., $n = 3$)

WSC/TPP (*w*/*w*)	Size (nm)		Zeta potential (mV)		Loading efficiency (%)
	Blank[a)]	BSA-loaded[b)]	Blank[a)]	BSA-loaded[b)]	
9:1	N.D.[c)]		N.D.[c)]		N.D.[c)]
10:1	113.5±9.2	135.5±10.2	35.2±1.5	31.2±2.9	68.1±2.3
14:1	82.5±10.1	99.7±9.4	37.3±3.1	34.2±4.6	25.2±3.3
18:1	67.8±9.7	110.2±11.3	39.3±2.7	38.1±3.1	12.9±1.8
20:1	35.6±10.2	55.1±8.7	41.8±3.6	39.2±2.1	4.7±0.7
21:1	N.D.[d)]		N.D.[d)]		N.D.[d)]

a) Blank nanoparticles; b) BSA-loaded nanoparticles; c) not determined, no nanoparticles formation because aggregation emerged; d) not determined, no nanoparticles formation because reaction solution was still clear. MW 6.3 kDa, BSA initial concentration 0.2 mg/mL, $T = 25\pm1$℃, pH = 7.4.

san-alginate microspheres[30]. Relatively low adhesivity of WSC with lower WSC/TPP weight ratio promotes association of BSA. Blank (without associated BSA) WSC/TPP nanoparticles displayed particle sizes in the range of approximately 35—120 nm and a positive zeta potential from 35 to 42 mV. Larger nanoparticles show a tendency for decreased zeta potential for BSA-loaded nanoparticles at a certain ratio of WSC/TPP[15].

3.2 BSA loading of nanoparticles

BSA loading efficiency and loading capacity were significantly affected by the initial BSA concentration (Figure 3), and the lower the concentration, the higher the loading efficiency which increased from 5% to 79%. However, by increasing the initial BSA concentration from 0.05 to 1 mg/mL, the protein loading capacity was enhanced from 3.5% to 14%. On the other hand, both BSA loading efficiency and loading capacity were decreased with the addition of PEG in WSC solution. As reported in ref. [31], the acid group of BSA and the oxygen atom of PEG may compete in their interaction with WSC amino groups, so the entanglement of PEG chains with the WSC molecules hinders the encapsulation of BSA into the nanoparticles.

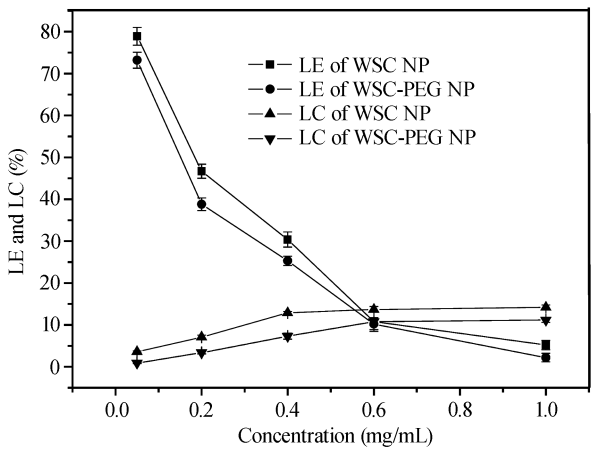

Figure 3 Effect of BSA initial concentration on BSA loading efficiency (LE) and loading capacity (LC) (MW 6.3 kDa, WSC 2 mg/mL, TPP 1 mg/mL, $n = 3$).

Figure 4 shows the influence of DD and MW of WSC on the BSA loading efficiency. As the DD of WSC (MW 6.3 kDa) increased, the loading efficiency increased similar to high molecular weight chitosan[26]. It can be deduced that WSC with higher DD contains more functional groups, which can complex with the acid groups of BSA and gelate with the tripolyphosphoric groups, so the loading efficiency of BSA increases correspondingly. On the other hand, the loading efficiency increased also as the MW of WSC (DD 90.7%) increased. Sabnis et al.[32] concluded that chitosan effectiveness in coagulated solids and proteins was inversely proportional to its MW. They observed that depolymerization of chitosan yielded a polymer with greater complexation capability due to an increase in the number of amino groups. But Flory[33] stated that in general, the intrinsic reactivity of all functional groups on a polymer remains the same. WSC with low molecular weights can easily dissolve in water and its molecular chains can unfold enough to avoid crystalline structure formation, so WSC with various MWs but the same DD has the same functional groups similar to Flory's statement. The loading efficiency of WSC with MW from 3.5 to 6.3 kDa increases dramatically from 8% to 48% but up to 15.8 kDa the increased tendency is slight. Xu et al.[26] stated that compared with the chitosan with smaller MW smaller than 68 kDa (the MW of BSA), encapsulation efficiency (equal to loading efficiency) of chitosan with greater MW than 68 kDa is much greater, and they supposed that this is attributed to their longer chains of the molecule which can entrap greater amount of BSA when they gelate with TPP. We disagree with their supposition because the loading efficiency of a WSC with much smaller MW than BSA's can show interesting loading efficiencies even when the MW of the WSC is down to mere 6.3 kDa.

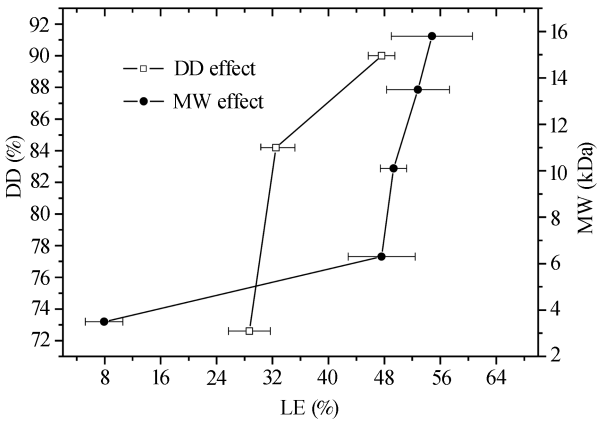

Figure 4 Effect of DD and MW of WSC on BSA loading efficiency (WSC 2 mg/mL, TPP 1 mg/mL BSA 0.1 mg/mL, WSC MW 6.3 kDa with different DD and WSC 90% DD with different MW were utilized, n=3).

3.3 *In vitro* release

The BSA *in vitro* release test for WSC or PEG-modified WSC nanoparticles proves that they have a sustained release form as shown in Figures 5—7. Similar to *in vitro* results reported previously about high MW chitosan nanoparticles[26], all release profiles of the nanopar-

ticles exhibited a small burst release of about 20% of total BSA amount in the first 12 h, and then a slow release at a constant rate. This suggests that WSC nanoparticles can adsorb BSA not only on their huge specific surface area but also in their pores, where the initial burst release of protein is associated with those protein molecules dispersing close to the microspheres surface, which easily diffuse out during the initial incubation time[34], and the slow release is attributed to those protein molecules cross-linked in the pores.

3.3.1 Effect of BSA loading and PEG presence. As shown in Figure 5, BSA release rate was influenced by the amount of protein loaded; a higher loading capacity provided a faster release rate. The different release rates between nanoparticles with 6.7% and 10.2% loading capacities are attributed to the BSA concentration gradient, where the release rate is usually drug concentration gradient driven, i.e. higher levels of loaded drug lead to a wider concentration gap between the polymeric nanoparticles and the release medium, which causes a higher diffusion rate. PEG presence accelerates BSA release as shown in Figure 5, and WSC/PEG nanoparticles with a loading capacity of 9.5% provide faster release rates than WSC nanoparticles with a loading capacity of 10.2%. This suggests that the entanglement of PEG chains with the chitosan molecules hinders the packed and rigid bonding between chitosan and BSA, so relatively loose structure of nanoparticles containing PEG results in a higher rate of BSA release.

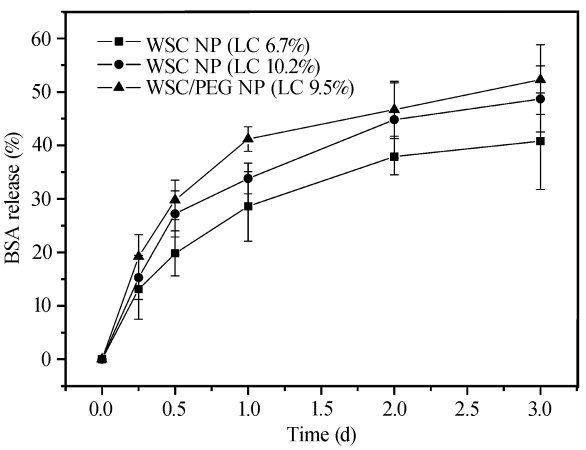

Figure 5 Effect of loading capacity and PEG presence on BSA release behavior (MW 6.3 kDa, DD 90.7%, *n*=3).

3.3.2 Effect of DD and MW. As shown in Figure 6, WSC with higher DD provided lower BSA release rates. Strong gelation and hydrogen bonding is formed in nanoparticles with high DD as revealed by the FTIR

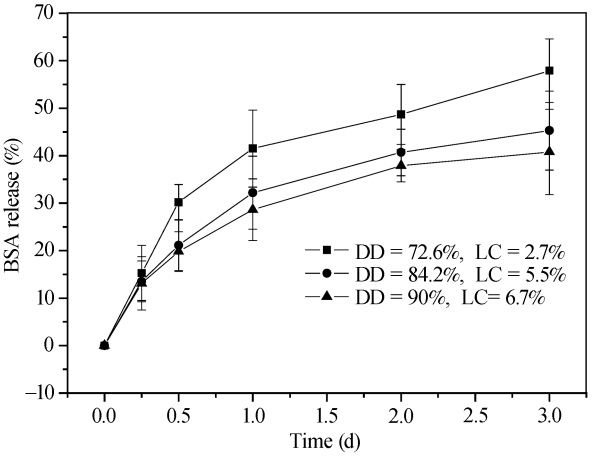

Figure 6 Effect of DD of WSC on BSA release behavior (MW = 6.3 kDa, *n*=3).

analysis of WSC matrix and nanoparticles. Higher DD of WSC with the same MW provides more compact nanoparticles due to the greater number of ammonium groups of WSC gelated with tripolyphosphoric groups, so the lower permeability of the nanoparticles surface results in a slow release rate.

As shown in Figure 7, WSC with higher MW has a lower release rate even if its loading capacity was relatively high. In three days, BSA release percents of nanoparticles with MWs of 3.5, 6.3, 10.1, 13.5 kDa were 89.8%, 43.8%, 40.2% and 37.5%, respectively. Among the four categories of MWs of WSC, the smallest MW of 3.5 kDa showed the fastest release rate which was overwhelmingly higher than all the others. As the MW of WSC increased from 6.3 to 13.5 kDa, the release rates decreased slightly and were closer to each other. The influence of MW of the polymer on nanoparticles surface permeability has not been reported, and the mechanism is not clear. However, the results in Figure 7 sug-

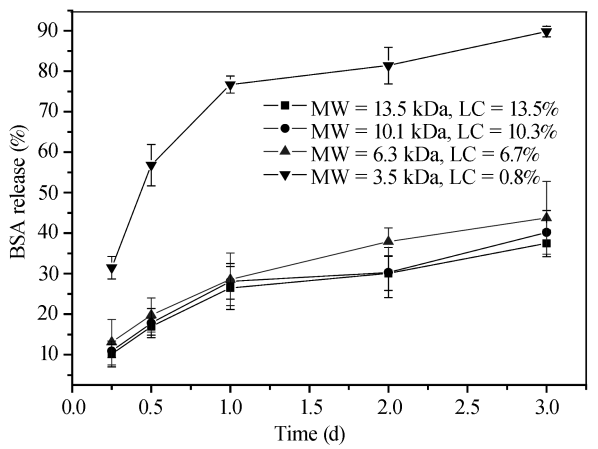

Figure 7 Effect of MW of WSC on BSA release behavior (WSC DD 90%, *n* =3).

gest that WSC with MW of 3.5 kDa was too small to load BSA molecules whereas MWs higher than 6.3 kDa load much more easily. Therefore, it could be hypothesized that the permeability of coacervated nanoparticle is lower with increasing MW due to denser chain packing and increased inter-chain bonding as well as from higher rigidity.

The authors are grateful for Tian Yingzi, Director, Autoszer and Wu Dongxiao, Director, TEM for extending help and for their continuous assistance throughout this study.

1 Thanou M, Verhoef J C, Junginger H E. Chitosan and its derivatives as intestinal absorption enhancers. Adv Drug Deliv Rev, 2001, 50(Suppl 1): 91－101
2 Dodane V, Vilivalam V D. Pharmaceutical applications of chitosan. Pharm Sci Technol Today, 1998, 1(6): 246－253
3 Felt O, Buri P, Gurny R. Chitosan: a unique polysaccharide for drug delivery. Drug Dev Ind Pharm, 1998, 24: 979－993
4 Kavashima Y, Lin SY, Kasai A, et al. Preparation of a prolonged release tablet of aspirin with chitosan. Chem Pharm Bull, 1985, 33: 2107－2113
5 Thanoo B C, Sunny M C, Jayakrishnan A. Crosslinked chitosan microspheres: preparation and evaluation as a matrix for the controlled release of pharmaceuticals. J Pharm Pharmacol, 1992, 44: 283－286
6 Akbuga J, The effect of physicochemical properties of a drug on its release from chitosan malate tablets. Int J Pharm, 1993, 100: 257－261
7 Tanima B, Susmita M, Ajay K S, et al. Preparation, characterization and biodistribution of ultrafine chitosan nanoparticles. Int J Pharm, 2002, 243(1-2): 93－105
8 Janes K A, Calvo P, Alonso M J. Polysaccharide colloidal particles as delivery systems for macromolecules. Adv Drug Deliv Rev, 2001, 47(1): 83－97
9 Kim T H, Park I K, Nah J W, et al. Galactosylated chitosan/DNA nanoparticles prepared using water-soluble chitosan as a gene carrier. Biomaterials, 2004, 25(17): 3783－3792
10 Ilyina A V, Tikhonov V E, Albulov A I, et al. Enzymic preparation of acid-free-soluble chitosan. Process Biochem, 2000, 35(6): 563－568
11 Qin C, Du Y, Xiao L, et al. Enzymic preparation of water-soluble chitosan and their antitumor activity. Int J Biol Macromol, 2002, 31(1-3): 111－117
12 Jang M K, Jeong Y I, Cho C S, et al. The preparation and characterization of low molecular and water soluble free-amine chitosan. Bull Korean Chem Soc, 2002, 23: 914－916
13 Chae S Y, Son S, Lee M, et al. Deoxycholic acid-conjugated chitosan oligosaccharide nanoparticles for efficient gene carrier. J Control Release, 2005, 109(1-3): 330－344
14 Vila A, Sánchez A, Janes K, et al. Low molecular weight chitosan nanoparticles as new carriers for nasal vaccine delivery in mice. Eur J Pharm, 2004, 57(1): 123－131
15 Fernàndez-Urrusuno R, Calvo P, Remunan-Lopez C, et al. Enhancement of nasal absorption of insulin using chitosan nanoparticles. Pharm Res, 1999, 16: 1576－1581
16 De Campos A M, Sánchez A, Alonso M J. Chitosan nanoparticles: a new vehicle for the improvement of the delivery of drugs to the ocular surface. Application to Cyclosporin A Int J Pharm, 2001, 224(1-2): 159－168
17 Gerf R, Minamitake Y, Perracchia M T, et al. Biodegradable long-circulating polymeric nanospheres. Science, 1994, 263: 1600－1603
18 Quellec P, Gref R, Perrin L, et al. Protein encapsulation within polyethylene glycol-coated nanospheres. I. Physicochemical characterization. J Biomed Mater Res, 1998, 42: 45－54
19 Peracchia M T, Gref R, Minamitake Y, et al. PEG-coated nanospheres from amphiphilic diblock and multiblock copolymers: Investigation of their drug encapsulation and release characteristics. J Control Rel, 1997, 46(3): 223－231
20 Calvo P, Remunan-López C, Vila-Jato J L, et al. Novel hydrophilic chitosan-polyethylene oxide nanoparticles as protein carriers. J Appl Pol Sci, 1997, 63(1): 125－132
21 Qin C, Xiao L, Du Y M. Antitumer activity of chitosan hydrogen selenties. Chin Chem Lett, 2002, 13: 213－214
22 George A F R, Frances A W. A study of the influence of structure on the effectiveness of chitosan as an antifelting treatment for wool. J Biotechnol, 2001, 89(2-3): 297－304
23 Wu Y, Yang W, Wang C, et al. Chitosan nanoparticles as a novel delivery system for ammonium glycyrrhizinate. Int J Pharm, 2005, 295(1-2): 235－245
24 Grenha A, Seijo B, Remuñán-López C. Microencapsulated chitosan nanoparticles for lung protein delivery. Eur J Pharm Sci, 2005, 25(4-5): 427－437
25 Chung H, Kim T W, Kwon M, et al. Oil components modulate physical characteristics and function of the natural oil emulsions as drug or gene delivery system. J Control Rel, 2001, 71(3): 339－350
26 Xu Y, Du Y. Effect of molecular structure of chitosan on protein delivery properties of chitosan nanoparticles. Int J Pharm, 2003, 250(1): 215－226
27 Xu Y, Du Y, Huang R, et al. Preparation and modification of *N*-(2-hydroxyl) propyl-3-trimethyl ammonium chitosan chloride nanoparticle as a protein carrier. Biomaterials, 2003, 24(27): 5015－5022
28 Knaul J Z, Hudson S M, Creber K A M. Improved mechanical properties of chitosan fibers. J Appl Polym Sci, 1999, 72: 1721－1731
29 Calvo P, Remuñan-López C, Vila-Jato J L, et al. Chitosan and chitosan/ethylene oxide-propylene oxide block copolymer nanoparticles as novel carriers for proteins and vaccines. Pharm Res, 1997, 14(10): 1431－1436
30 Vandenberg G W, Drolet C, Scott S L, et al. Factors affecting protein release from alginate-chitosan coacervate microcapsules during production and gastric/intestinal simulation. J Control Rel, 2001, 77(3): 297－307
31 Kim S S, Lee Y M. Synthesis and properties of semi-interpenetrating polymer networks composed of β-chitin and poly (ethylene glycol) macromer. Polymer, 1995, 36(23): 4497－4501
32 Sabnis S S, Block L H. Chitosan as an enabling excipient for drug delivery systems 1. molecular modifications. Int J Biol Macromol, 2000, 27(3): 181－186
33 Flory P J. Principles of Polymer Chemistry. New York: Cornell University Press, 1953. 69
34 Zhou S B, Deng X M, Li X H. Investigation on a novel core-coated microspheres protein delivery system. J Control Rel, 2001, 75(1-2): 27－36